UNIVERSITY OF CALIFORNIA, SAN DIEGO

A Search for New Physics using the $M_{\mathbf{T2}}$ Stransverse-Mass Variable in All-Hadronic Final States produced in proton-proton Collisions with a Center of Mass Energy of 13 TeV

A dissertation submitted in partial satisfaction of the
requirements for the degree
Doctor of Philosophy

in

Physics

by

Mark Derdzinski

Committee in charge:

Professor Frank Würthwein, Chair
Professor Avraham Yagil
Professor Benjamin Grinstein
Professor Farhat Beg
Professor Ian Galton

2018

The dissertation of Mark Derdzinski is approved, and it is acceptable in quality and form for publication on microfilm and electronically:

_____

_____

_____

_____

_____

Chair

University of California, San Diego

2018

DEDICATION

Dedication here.

EPIGRAPH

For knowledge comes slowly, and when it comes, it is often at great personal expense.

— Paul Auster, *Ghosts*

TABLE OF CONTENTS

LIST OF FIGURES

LIST OF TABLES

ACKNOWLEDGEMENTS

Acknowledgements

VITA

2011	B. A. in Physics and Mathematics, University of California, Berkeley
2014	M. S. in Physics, University of California, San Diego
2018	Ph. D. in Physics, University of California, San Diego

PUBLICATIONS

Search for new physics with the M_{T2} variable in all-jets final states produced in pp collisions at $\sqrt{s} = 13$ TeV, *The CMS collaboration, Khachatryan, V., Sirunyan, A.M. et al.* J. High Energ. Phys. (2016) 2016: 6. doi:10.1007/JHEP10(2016)006 `arXiv:1603.04053 [hep-ex]`

Search for new physics in the one soft lepton final state using 2015 data at $\sqrt{s} = 13$ TeV, *CMS Collaboration*, Physics Analysis Summary (2016), CMS-PAS-SUS-16-011

ABSTRACT OF THE DISSERTATION

A Search for New Physics using the $M_{\mathbf{T2}}$ Stransverse-Mass Variable in All-Hadronic Final States produced in proton-proton Collisions with a Center of Mass Energy of 13 TeV

by

Mark Derdzinski

Doctor of Philosophy in Physics

University of California, San Diego, 2018

Professor Frank Würthwein, Chair

Abstract.

Chapter 1

Introduction

Chapter 2

The Large Hadron Collider and the CMS Detector

2.1 The Large Hadron Collider

2.2 The Compact Muon Solenoid

The Compact Muon Solenoid (CMS) is a general-purpose physics detector at the LHC, situated at one of the five collision points along the main ring. The detector encapsulates the collision point with layers of various subsystems designed to interact with the outgoing particles of the proton-proton collisions, and measure the position and energies of the collision products. Because of the extremely high rate of interactions at the collision point **FIXME: add specifics about number of collisions per second and ave collisions per crossing?**, saving data from every bunch crossing would be unsustainable,

and so the detector is also equipped with a system of hardware and software implemented "triggers" which identify events of interest for physics analyses to be saved to disk for further analysis.

The physical construction of the detector is motivated by the different interaction of particles with different types of materials, and consists of several subsystems layered as coaxial cylinders around the interaction point. Each subsystem consists of (sometimes different) components covering the fiducial area coaxial with the beamline (the "barrel") and also the ends of the cylinder (the "endcaps"). The innermost subsystem of CMS is the silicon tracker, which consists of many layered silicon pixels designed to pinpoint the locations of charged particles while minimally interacting with the particle's trajectory. The layer beyond the tracker is the electromagnetic calorimeter (ECAL), a grid of lead-tungstate crystals which scintillate to measure the energies of electromagnetic particles. Beyond the ECAL is the hadronic calorimeter (HCAL), a sampling calorimeter designed to measure the energies of hadronic particles (which deposit minimal energy in the ECAL). The final, outer layer is the CMS muon detector, where the muon detection stations are interweaved with the magnetic return yoke that generates the toroidal 3.8T magnetic field inside the detector volume. The total dimensions of the detector are **FIXME: cms actual size**.

2.2.1 Silicon Vertex Tracker

The silicon vertex tracker (SVT) is a series of silicon pixels and strips designed to measure the position of charged particles in the detector, while disturbing their path as

little as possible. The position of particles in the interior is of particular importance in event reconstruction; charged particles traveling in a magnetic field will deflect in a curved path with radius proportional to the particles momentum as described in equation 2.1, and so the track reconstruct can be used to not only determine a particle's momentum with high precision, but also the sign of its charge based on the direction of curvature.

$$p = qrB \tag{2.1}$$

As the innermost detector subsystem, the SVT experiences the highest flux of particle radiation. In the barrel region, the tracker layers are oriented in 3 coaxial layers. Closest to the interaction point where particle flux is the greatest, very precise silicon pixels are used, measuring $100 \times 150 \mu\text{m}^2$, whereas in other layers the flux is low enough to use microstrip detectors, measuring $10\text{cm} \times 80\mu\text{m}$ and $25\text{cm} \times 180\mu\text{m}$ in the middle and outer layers respectively. In the endcaps, the pixel strips are arranged in a turbine-like pattern in two separate layers on each end. This configuration allows for the precise measurement of particle position for track reconstruction, while minimizing the amount of material which might deflect particles from their original trajectories.The geometry of the SVT layout can be seen in figure 2.1.

2.2.2 Electromagnetic Calorimeter

The ECAL is used to measure the energies of particles which interact electromagnetically, both absorbing the incident particles and scintillating to provide an energy-readout to photodiodes attached to each crystal. Constructed of lead-tungstate ($PbWO_4$), elec-

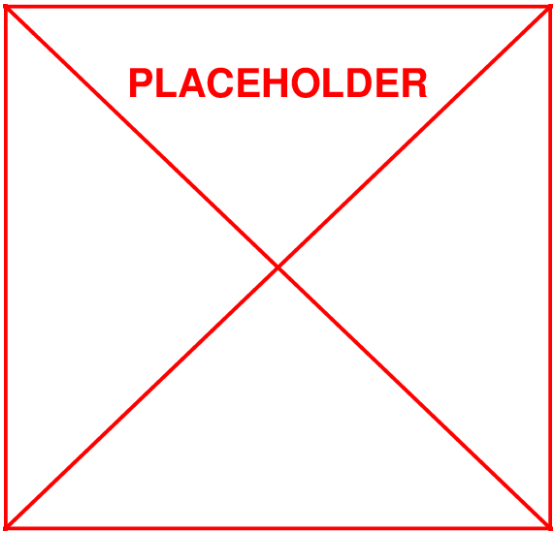

Figure 2.1: Geometry of silicon tracker layers in CMS.

tromagnetically interacting particles (such as electrons or photons) will interact with the crystal material, losing energy through a cascade of electromagnetic interactions including election-positron pair production and bremsstrahlung, as pictured in figure 2.2. This phenomenon — also referred to as "showering" — causes the crystals to scintillate proportional to the energy deposited in the crystal, which is then measured by various photodiodes to extract an accurate measurement of the particle energy, now fully absorbed by the calorimeter.

The fundamental principle of the calorimeter measurement relies on the energy loss of particles interacting with matter. In general, the energy of a particle traveling a distance X through some material is given by equation 2.2, where E_0 is the initial energy of the particle and X_0 is the material-dependent radiation length. The design of the calorimeter is motivated by the choice of a scintillating, radiation-hard material with short X_0 such that incident electromagnetic particles deposit all their energy and are stopped by the ECAL.

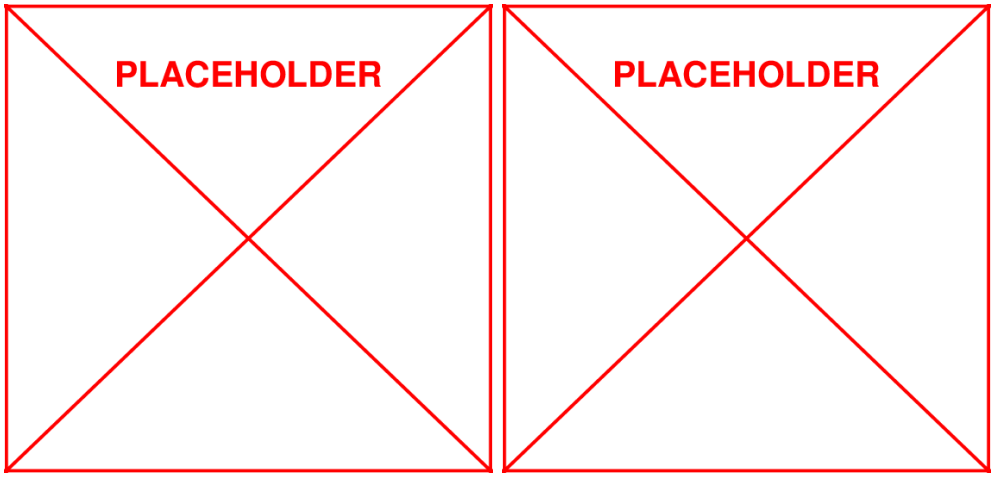

Figure 2.2: Feynman diagrams depicting the main processes by which particles shower in the ECAL. The left diagram depicts electron-positron pair production from a photon, and the right diagram depicts bremsstrahlung, where an electron radiates energy away through a photon.

The resolution of the energy measurement is also dependent on the "stochastic term", which parametrizes the uncertainty due to statistical and measurement fluctuations in the calorimeter,and is given by equation 2.3, where S is the stochastic term, N the noise, and C the constant term. The energy resolution can be measured by a test beam of known energy, as shown in figure 2.3.

$$E(x) = E_0 e^{\frac{-x}{X_0}} \tag{2.2}$$

$$\left(\frac{\sigma}{E}\right)^2 = \left(\frac{S}{\sqrt{E}}\right)^2 + \left(\frac{N}{E}\right)^2 + C^2 \tag{2.3}$$

The construction of the calorimeter is also divided into two sections by the cylindrical geometry, the ECAL barrel section (EB) and ECAL endcap sections (EE). The EB

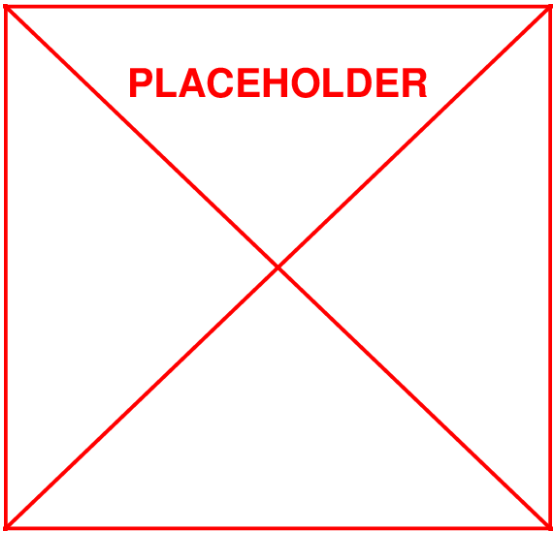

Figure 2.3: Energy resolution σ/E of the ECAL as a function of electron energy measured using a test beam. The energy was measured in a 3×3 crystal array with electrons incident on the center crystal, with electrons falling in a $4 \times 4\text{mm}^2$ region (lower points) and $20 \times 20\text{mm}^2$ region (upper points).

consists of 61,200 crystals arranged into 36 "supermodules", each spanning half the barrel length, and uses silicon avalanche photodiodes (APDs) as photodetectors. The individual crystals are tilted slightly (3°) in an $\eta - \phi$ grid with respect to the nominal interaction point, with a front-facing area of $22 \times 22\text{mm}^2$ and a length of 230mm. The EE instead uses vacuum phototriodes (VPTs) as photodetectors, and consists of approximately 15,000 crystals clustered in 5×5 units, also offset from the interaction point but arranged in an $x - y$ grid, with a cross section of $28.6 \times 28.6\text{mm}^2$ and a length of 220mm. The EE is also equipped with a "preshower" device placed in front of the crystal calorimeter, consisting of two strips of silicon strip detectors to enhance π^0 rejection. The layout of the ECAL can be seen in figure 2.4. Because of the depth of the ECAL crystals (which are $\tilde{2}5X_0$, and the confining properties of the crystals (which have a Moliere radius of 2.2cm, the radius of a cylinder containing 90% of a shower's energy on average), electrons and photons are typically well reconstructed in CMS, except in the transition region where EB and EE meet.

2.2.3 Hadronic Calorimeter

The CMS HCAL is a sampling calorimeter. Designed with alternating layers of scintillating and absorbing material, incident hadronic particles (such as charged pions, kaons, protons, etc.) interact with the absorber material and consequently shower into electromagnetic particles, whose energy can be read out by photodiodes connected to the scintillating material. Brass is used as the absorber material for both its interaction length and non-magnetic properties, and plastic scintillator tiles connected to embedded

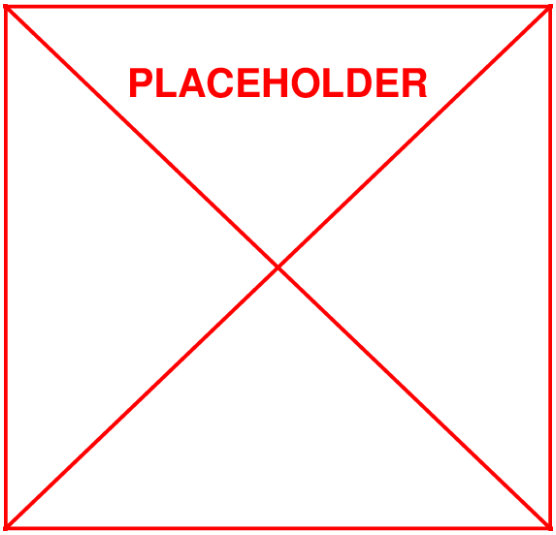

Figure 2.4: A cross section of the ECAL geometry, with the dashed lines marking the pseudorapidity values η covered by the various subsystems.

wavelength-shifting fibers carry the light to a readout system.

2.2.4 Muon Detectors

2.3 CMS Physics Objects

Chapter 3

The $M_{\mathbf{T2}}$ Variable Search

3.1 Analysis Strategy

Searches for new physics targeting all-hadronic final states present unique challenges and opportunities at the LHC. While such searches typically implement stringent vetoes on lepton candidates and thus bypass the need to correctly identify "real" leptons from similar signals in the detector, the high rate of QCD processes in proton-proton collisions generates large amounts of SM events (with all-hadronic final states). Designing a search targeting signatures with all-hadronic final states thus requires a mechanism to distinguish and suppress the selection of SM-QCD events from new physics signatures, as well as robust background estimation methods to predict the yield of standard model events which may generate a momentum imbalance in the detector reconstruction of the event (such as $Z \to \nu\nu$).

The M_{T2} analysis harnesses the discriminating power of the M_{T2} stransverse mass

variable to distinguish standard model events from possible signatures including new physics. By first requiring a nominal amount of missing energy in the event, SM-QCD processes are greatly suppressed (since missing energy is not due to physics processes but detector reconstruction or mis-measurement of the underlying event). Additional requirements on the topology of the event (implemented using M_{T2}) further suppress QCD-like processes and favor events with real missing energy anti-aligned with the all-hadronic energy deposits in the detector. After estimating the minimal QCD contribution remaining by extrapolating from a region orthogonal to the signal selection, the only remaining backgrounds are leptonic events where the lepton was failed to be constructed or identified (or "lost-lepton" events), and SM events where energy escapes the detector in the form of neutrinos from a decaying Z boson recoiling against jets (or "invisible Z" events).

3.2 Event Selection Criteria

The general strategy for the event selection is to first apply baseline cuts on motivated by hardware and software-level triggers **FIXME: call back to trigger section in previous chapter? or explain triggers** and reducing the QCD multi-jet background to negligible levels. Events are further categorized using the scalar sum of the transverse momenta p_{T} of all selected jets (H_{T}), the total number of jets in the event (N_{jets}), the total number of b-tagged jets in the event ($N_{\mathrm{b\text{-}jets}}$), and M_{T2} . Events are reconstructed with the CMS particle-flow (PF) algorithm **FIXME: cite PF**, which is designed to holistically use all event information from each detector element to reconstruct and identify

each particle in the event (hereafter referred to as "PF candidates"). A summary of the event preselections can be found in **FIXME: cite table with preselections**.

3.3 Search Regions

3.4 Control Regions

Bibliography